Ramped Temperature Effect on Unsteady MHD Natural Convection Flow Past an Infinite Inclined Plate in the Presence of Radiation, Heat Source and Chemical Reaction

[1]M. NARAHARI, [2]SOWMYA TIPPA, [3]RAJASHEKHAR PENDYALA, [4]M. YUNUS NAYAN
[1]Petroleum Engineering Department
[2, 4]Fundamental and Applied Sciences Department
[3]Chemical Engineering Department
Universiti Teknologi PETRONAS
32610 Bandar Seri Iskandar, Perak
MALAYSIA
[1]marneni@petronas.com.my; [2]t.sowmya88@gmail.com; [3]rajashekhar_p@petronas.com.my;
[4]yunusna@petronas.com.my

Abstract: - An analytical investigation of the effects of magnetic field, thermal radiation, heat generation or absorption and chemical reaction on the unsteady natural convection flow along an infinite inclined plate embedded in a porous medium subject to a ramped temperature boundary condition is performed. The governing equations for momentum, energy and concentration have been solved using the Laplace transform technique. The closed form exact solutions for the velocity, temperature and concentration fields as well as skin friction, Nusselt and Sherwood numbers are obtained without any restrictions. The influence of temporal variable, inclination angle, buoyancy ratio, permeability, magnetic field, heat generation or absorption, thermal radiation, Schmidt number and chemical reaction on the dimensionless velocity and skin-friction has been discussed through graphs. The natural convection due to ramped wall temperature has also been compared with that of the isothermal plate. It is found that the velocity and skin friction decreases with increasing radiation parameter, magnetic field parameter and angle of inclination in both ramped and isothermal cases.

Key-Words: - Free convection, chemical reaction, thermal radiation, inclined plate, porous medium, magnetohydrodynamics (MHD), ramped temperature, heat generation or absorption.

1 Introduction

Fluid flow and the combined heat and mass transfer along an inclined plate have received less attention than the cases of vertical and horizontal plates. This configuration is very frequently encountered in numerous applications such as solar energy systems, geophysics, materials processing etc., and in the natural environment. Most of the previous studies were investigated by either numerical simulations or experimental observations. Practical problems often involve wall conditions that are non-uniform or arbitrary. To understand such problems, it is useful to investigate problems which are subjected to step change in wall temperature. Several attempts in this direction were made by various authors. Lee and Yovanovich [1] studied the laminar natural convection heat transfer from a vertical flat plate with discontinuous wall temperature using a new analytical model and the results obtained were compared with the existing numerical data of Hayday et al. [2] and the perturbation series solution of Kao [3]. The unsteady free convective flow of an incompressible viscous fluid near a vertical plate with ramped wall temperature was analyzed by Chandran et al. [4] by using the Laplace transform technique and the results were compared with that of the isothermal plate. Narahari and Dutta [5] analytically studied the problem of free convection flow induced by the heat and mass transfer along an accelerated infinite vertical plate with ramped wall temperature. An exact solution to the unsteady natural convection flow of a viscous incompressible fluid in a vertical channel due to ramp heating at one boundary was reported by Narahari and Raghavan [6] with the help of Laplace transform technique. The influence of constant mass transfer and constant mass flux on free convection flow past an infinite vertical plate with ramped temperature was investigated by Narahari et al [7]. They observed that the fluid velocity is greater in the case of an isothermal plate than that of the ramped temperature plate for both constant mass transfer and constant mass flux

boundary conditions. Saha et al. [8] studied the two dimensional transient natural convection flows adjacent to a sudden and ramp heated inclined flat plate using the scaling analysis and numerical simulations.

Radiation effects on free convection flow past an inclined/vertical surface with a step change in wall temperature are also important in the processes involving high temperatures in some industrial and technological applications such as glass production, furnace design, heating and cooling chambers, plasma physics, solar energy collector and power generation systems. Additionally, the use of electrically conducting fluid under the influence of magnetic field has gained great interest in the study of boundary-layer flows. The effect of ramped temperature on the unsteady MHD free convective flow of an incompressible, electrically conducting fluid in a porous medium bounded by an infinite vertical wall was analytically investigated by Tiwari [9]. The effect of a transverse magnetic field on the two-dimensional unsteady natural convective flow of an electrically conducting and viscous incompressible fluid past a semi-infinite vertical plate was studied numerically by Singh and Singh [10] when the temperature of the plate has temporally ramped continuous profiles. The influence of thermal radiation on unsteady hydromagnetic natural convection flow of a viscous incompressible electrically conducting fluid near an impulsively started vertical plate with ramped temperature in a porous medium was investigated by Seth et al. [11] with the help of Laplace transform technique. The numerical analysis of the effects of thermal radiation and chemical reaction on the transient MHD free convection mass transfer flow of a dissipative fluid past an infinite vertical porous plate subject to a ramped wall temperature was investigated by Rajesh [12] using Crank-Nicolson finite difference method. Kalidas [13] studied the effects of thermal radiation and chemical reaction on unsteady MHD free convection heat and mass transfer flow of a viscous incompressible electrically conducting fluid near an impulsively moving vertical flat plate with ramped wall temperature. Exact solutions of this problem were obtained in closed form by using Laplace transform technique. The closed form analytical solutions were derived by Narahari [14] to examine the transient free convection flow between long vertical parallel plates with ramped wall temperature at one boundary in the presence of thermal radiation and constant mass diffusion by using Laplace transform technique. Samiulhaq et al. [15] investigated the unsteady MHD natural convection flow of an incompressible viscous fluid past an impulsively started infinite vertical plate in a porous medium with ramped temperature profile in the presence of radiation and Soret effects. Narahari and Sulaiman [16] performed an analytical study to investigate the effects of thermal radiation and magnetic field on the unsteady natural convection flow past an infinite inclined plate with ramped temperature using the Laplace transform technique. The effects of suction/blowing and mass transfer on the unsteady hydromagnetic free convective flow of a viscous, incompressible, electrically conducting and radiating fluid past a porous flat plate with ramped wall temperature in the presence of chemical reaction was investigated by Nandkeolyar et al. [17] by using the Laplace transform technique. Recently, Ismail et al. [18] performed an analytical study by using Laplace transform technique for the unsteady magnetohydrodynamic free convection flow in a porous medium past an infinite inclined plate with ramped temperature in the presence of thermal radiation. However, the unsteady free convection flow of an optically thin gray gas past an infinite inclined plate with ramped temperature embedded in a porous medium under the influence of magnetic field, thermal radiation, heat generation or absorption and the first-order chemical reaction has not been addressed in the literature even though this problem finds potential applications in the design of solar energy collectors, geothermal energy systems, cooling of nuclear reactors and in the design of heat exchangers.

In the present paper, the effects of transverse magnetic field, thermal radiation, heat generation or absorption and first-order chemical reaction on the unsteady free convection flow past an infinite inclined plate in a porous medium with ramped wall temperature have been investigated. The governing partial differential equations are solved analytically using the Laplace transform technique without any restriction and closed form solutions are obtained for the velocity, temperature and concentration fields, skin-friction, Nusselt and Sherwood numbers. These solutions can be used as a benchmark for the comparison of numerical simulations of higher order models and experimental investigations.

2. Governing Equations and Solutions

Consider the unsteady laminar heat and mass transfer by natural convection along an infinite inclined plate through a porous medium. The x'-

axis is taken along the plate with the angle of inclination ϕ to vertical and the y'- axis is taken normal to the plate. Initially at $t' \le 0$, the plate and the fluid are at the temperature T'_∞ and concentration C'_∞. At $t' > 0$, the plate temperature increases according to the equation $T' = T'_\infty + (T'_w - T'_\infty)t'/t_0$ and the chemical species concentration raised to C'_w. It is assumed that the plate is electrically non-conducting and a magnetic field of uniform strength B_0 is applied in the y'-direction. The fluid is assumed to be optically thin, constant property radiating gas except the density variation in the body force term of the balance of linear momentum equation and it is also assumed that the radiation heat flux in the x'- direction is negligible as compared to that in the y'- direction. Since, the plate is assumed to be infinitely long in x' - axis direction so that all the dependent variables are functions of y' and t' only. Under the usual Boussinesq approximation, after neglecting heat due to viscous dissipation, the governing equations for the momentum, energy and solute concentration can be written as follows:

$$\frac{\partial u'}{\partial t'} = \nu \frac{\partial^2 u'}{\partial y'^2} + g\beta(T' - T'_\infty)\cos\phi + g\beta^*(C' - C'_\infty)\cos\phi - \nu \frac{u'}{K'_1} - \frac{\sigma B_0^2}{\rho} u' \tag{1}$$

$$\rho C_p \frac{\partial T'}{\partial t'} = k \frac{\partial^2 T'}{\partial y'^2} - q_c(T' - T'_\infty) - \frac{\partial q_r}{\partial y'} \tag{2}$$

$$\frac{\partial C'}{\partial t'} = D \frac{\partial^2 C'}{\partial y'^2} - \kappa(C' - C'_\infty) \tag{3}$$

with the following initial and boundary conditions

$$\left.\begin{aligned} & t' \le 0 : \; u' = 0, T' = T'_\infty, C' = C'_\infty \qquad \text{for all } y' \ge 0, \\ & t' > 0 : \begin{cases} u' = 0, \\ T' = \begin{cases} T'_\infty + (T'_w - T'_\infty)\, t'/t_0, & 0 < t' \le t_0 \\ T'_w, & t' > t_0 \end{cases} \\ C' = C'_w \end{cases} \text{at } y' = 0, \\ & u' \to 0, T' \to T'_\infty, C' \to C'_\infty \qquad \text{as } y' \to \infty. \end{aligned}\right\} \tag{4}$$

For an optically thin constant property gas, the radiative heat flux q_r satisfies the following non-linear differential equation:

$$\frac{\partial q_r}{\partial y'} = 4\alpha\sigma^*\left(T'^4 - T'^4_\infty\right) \tag{5}$$

where α is the absorption coefficient and σ^* is the Stefan-Boltzmann constant. It is assumed that the temperature differences within the flow are sufficiently small such that T'^4 may be expressed as a linear function of the fluid temperature T' using the Taylor series about T'_∞. After neglecting higher-order terms, gives

$$T'^4 \cong 4T'^3_\infty T' - 3T'^4_\infty . \tag{6}$$

Using Eqs. (5) and (6), Eq. (2) becomes

$$\rho C_p \frac{\partial T'}{\partial t'} = k \frac{\partial^2 T'}{\partial y'^2} - q_c(T' - T'_\infty) - 16\alpha\sigma^* T'^3_\infty (T' - T'_\infty) \tag{7}$$

The following non-dimensional quantities are introduced:

$$\left.\begin{aligned} & y = \frac{y'}{\sqrt{\nu t_0}}, t = \frac{t'}{t_0}, u = \frac{u'\sqrt{t_0}}{Gr\sqrt{\nu}}, \theta = \frac{T' - T'_\infty}{T'_w - T'_\infty}, \\ & C = \frac{C' - C'_\infty}{C'_w - C'_\infty}, Gr = \frac{g\beta(T'_w - T'_\infty)t_0^{3/2}}{\sqrt{\nu}}, \\ & Gm = \frac{g\beta^*(C'_w - C'_\infty)t_0^{3/2}}{\sqrt{\nu}}, N = \frac{Gm}{Gr}, \\ & K = \frac{K'_1}{\nu t_0}, M = \frac{\sigma B_0^2 t_0}{\rho}, \Pr = \frac{\mu C_p}{k}, Q = \frac{q_c \nu t_0}{k}, \\ & R = \frac{16\alpha\sigma^* \nu t_0 T'^3_\infty}{k}, \mathrm{Sc} = \frac{\nu}{D}, \gamma = \kappa t_0 . \end{aligned}\right\} \tag{8}$$

where u' is the fluid velocity in the x'-direction, t' is the time, ν is the kinematic viscosity, g is the acceleration due to gravity, β is the volumetric coefficient of thermal expansion, T' is the fluid temperature, T'_∞ is the temperature of the fluid away from the plate, β^* is the volumetric coefficient of concentration expansion, C' is the species concentration, C'_∞ is the species concentration away from the plate, K'_1 is the permeability of the porous medium, σ is the electrical conductivity of the fluid, ρ is the density, C_p is the specific heat at constant pressure, k is

ISBN: 978-1-61804-304-7

the thermal conductivity, q_c is the volumetric heat generation or absorption, q_r is the radiative heat flux in y'-direction, D is the mass diffusivity, κ is the chemical reaction parameter, T_w' is the temperature of the plate, and C_w' is the species concentration at the plate, y is the dimensionless coordinate axis normal to the plate, t is the dimensionless time, u is the dimensionless velocity, Gr is the thermal Grashof number, θ is the dimensionless temperature, C is the dimensionless species concentration, Gm is the mass Grashof number, N is the mass to thermal buoyancy ratio parameter, K is the dimensionless permeability parameter, M is the magnetic field parameter (square of the Hartmann number), μ is the fluid viscosity, Pr is the Prandtl number, Q is the heat generation or absorption parameter, R is the radiation parameter, Sc is the Schmidt number and γ is the dimensionless chemical reaction parameter.

From the above non-dimensional quantities, the ramp time t_0 can be defined as

$$t_0 = \frac{\nu^{1/3}}{g^{2/3}} \tag{9}$$

In view of Eqs. (8), Eqs. (1), (7), and (3) reduces to the following non-dimensional form, respectively,

$$\frac{\partial u}{\partial t} = \frac{\partial^2 u}{\partial y^2} + \theta\cos\phi + NC\cos\phi - \left(\frac{1}{K} + M\right)u \tag{10}$$

$$\mathrm{Pr}\frac{\partial \theta}{\partial t} = \frac{\partial^2 \theta}{\partial y^2} - (Q+R)\theta \tag{11}$$

$$\mathrm{Sc}\frac{\partial C}{\partial t} = \frac{\partial^2 C}{\partial y^2} - \mathrm{Sc}\gamma C \tag{12}$$

with the following initial and boundary conditions:

$$\left.\begin{aligned} &t \le 0: \ u = 0, \theta = 0, C = 0 \text{ for all } y \ge 0, \\ &t > 0: \begin{cases} u = 0, \theta = \begin{cases} t, & 0 < t \le 1 \\ 1, & t > 1 \end{cases}, C = 1 \text{ at } y = 0, \\ u \to 0, \theta \to 0, C \to 0 \text{ as } y \to \infty. \end{cases} \end{aligned}\right\} \tag{13}$$

Equations (10), (11) and (12) are solved exactly subject to the initial and boundary conditions (13) by the usual Laplace transform method without any restrictions and the solutions obtained for different cases are given below:

$$C(y,t) = F_2\left(y\sqrt{\mathrm{Sc}}, \gamma, 0, t\right) \tag{14}$$

$$\begin{aligned} \theta(y,t) = {} & F_1\left(y\sqrt{\mathrm{Pr}}, a_1, t\right) \\ & - F_1\left(y\sqrt{\mathrm{Pr}}, a_1, t-1\right)H(t-1) \end{aligned} \tag{15}$$

Case I: $\mathrm{Pr} \neq 1, \mathrm{Sc} \neq 1$

$$\begin{aligned} u(y,t) = {} & a_4\left[F_1(y,a_0,t) - F_1(y,a_0,t-1)H(t-1)\right. \\ & \left. - F_1(y\sqrt{\mathrm{Pr}},a_1,t) + F_1(y\sqrt{\mathrm{Pr}},a_1,t-1)H(t-1)\right] \\ & + a_5\left[F_2(y,a_0,0,t) - F_2(y,a_0,0,t-1)H(t-1)\right. \\ & - F_2(y\sqrt{\mathrm{Pr}},a_1,0,t) + F_2(y\sqrt{\mathrm{Pr}},a_1,0,t-1)H(t-1) \\ & - F_2(y,a_0,a_2,t) + F_2(y,a_0,a_2,t-1)H(t-1) \\ & + F_2(y\sqrt{\mathrm{Pr}},a_1,a_2,t) \\ & \left. - F_2(y\sqrt{\mathrm{Pr}},a_1,a_2,t-1)H(t-1)\right] \\ & + a_6\left[F_2(y,a_0,0,t) - F_2(y,a_0,a_3,t)\right. \\ & \left. - F_2(y\sqrt{\mathrm{Sc}},\gamma,0,t) + F_2(y\sqrt{\mathrm{Sc}},\gamma,a_3,t)\right] \end{aligned} \tag{16a}$$

Case II: $\mathrm{Pr} = 1, \mathrm{Sc} \neq 1$

$$\begin{aligned} u(y,t) = {} & a_4\left[F_1(y,a_0,t) - F_1(y,a_0,t-1)H(t-1)\right. \\ & \left. - F_1(y,a_7,t) + F_1(y,a_7,t-1)H(t-1)\right] \\ & + a_6\left[F_2(y,a_0,0,t) - F_2(y,a_0,a_3,t)\right. \\ & \left. - F_2(y\sqrt{\mathrm{Sc}},\gamma,0,t) + F_2(y\sqrt{\mathrm{Sc}},\gamma,a_3,t)\right] \end{aligned} \tag{16b}$$

Case III: $\mathrm{Pr} \neq 1, \mathrm{Sc} = 1$

$$\begin{aligned} u(y,t) = {} & a_4\left[F_1(y,a_0,t) - F_1(y,a_0,t-1)H(t-1)\right. \\ & \left. - F_1(y\sqrt{\mathrm{Pr}},a_1,t) + F_1(y\sqrt{\mathrm{Pr}},a_1,t-1)H(t-1)\right] \\ & + a_5\left[F_2(y,a_0,0,t) - F_2(y,a_0,0,t-1)H(t-1)\right. \\ & - F_2(y\sqrt{\mathrm{Pr}},a_1,0,t) + F_2(y\sqrt{\mathrm{Pr}},a_1,0,t-1)H(t-1) \\ & - F_2(y,a_0,a_2,t) + F_2(y,a_0,a_2,t-1)H(t-1) \\ & + F_2(y\sqrt{\mathrm{Pr}},a_1,a_2,t) \\ & \left. - F_2(y\sqrt{\mathrm{Pr}},a_1,a_2,t-1)H(t-1)\right] \\ & + a_8\left[F_2(y,a_0,0,t) - F_2(y,\gamma,0,t)\right] \end{aligned} \tag{16c}$$

where

$$a_0 = \frac{1}{K} + M, a_1 = \frac{(Q+R)}{\mathrm{Pr}}, a_2 = \frac{(Q+R-a_0)}{(1-\mathrm{Pr})},$$

ISBN: 978-1-61804-304-7

$$a_3 = \frac{(\mathrm{Sc}\gamma - a_0)}{(1-\mathrm{Sc})}, a_4 = \frac{\cos\phi}{(Q+R-a_0)},$$

$$a_5 = \frac{(1-\mathrm{Pr})\cos\phi}{(Q+R-a_0)^2}, a_6 = \frac{N\cos\phi}{(\mathrm{Sc}\gamma - a_0)},$$

$$a_7 = Q+R, a_8 = \frac{N\cos\phi}{\gamma - a_0},$$

$$F_1(z_1,z_2,t) = \left(\frac{t}{2} - \frac{z_1}{4\sqrt{z_2}}\right)\exp\left(-z_1\sqrt{z_2}\right)\times$$
$$\mathrm{erfc}\left(\frac{z_1}{2\sqrt{t}} - \sqrt{z_2 t}\right) + \left(\frac{t}{2} + \frac{z_1}{4\sqrt{z_2}}\right)\exp\left(z_1\sqrt{z_2}\right)\times$$
$$\mathrm{erfc}\left(\frac{z_1}{2\sqrt{t}} + \sqrt{z_2 t}\right),$$

$$F_2(z_1,z_2,z_3,t) = \frac{\exp(z_3 t)}{2}\left[\exp\left(-z_1\sqrt{z_2+z_3}\right)\times\right.$$
$$\mathrm{erfc}\left(\frac{z_1}{2\sqrt{t}} - \sqrt{(z_2+z_3)t}\right)$$
$$\left.+\exp\left(z_1\sqrt{z_2+z_3}\right)\mathrm{erfc}\left(\frac{z_1}{2\sqrt{t}} + \sqrt{(z_2+z_3)t}\right)\right],$$

z_1, z_2 and z_3 are dummy variables. Also, the following well known formula is used for complex error function.

$$\begin{aligned}\mathrm{erf}(a+ib) &= \mathrm{erf}(a) + \frac{\exp(-a^2)}{2\pi a}\times \\ &\left[1-\cos(2ab)+i\sin(2ab)\right] \\ &+ \frac{2\exp(-a^2)}{\pi}\sum_{n=1}^{\infty}\frac{\exp(-n^2/4)}{(n^2+4a^2)}\times \\ &\left[f_n(a,b)+ig_n(a,b)\right]+\varepsilon(a,b)]\end{aligned} \tag{17}$$

where

$$\begin{aligned}f_n(a,b) &= 2a - 2a\cosh(nb)\cos(2ab) \\ &\quad + n\sinh(nb)\sin(2ab), \\ g_n(a,b) &= 2a\cosh(nb)\sin(2ab) \\ &\quad + n\sinh(nb)\cos(2ab), \\ |\varepsilon(a,b)| &\approx 10^{-16}|\mathrm{erf}(a+ib)|.\end{aligned}$$

From the velocity field, the expression for skin-friction is derived and is given by

Case I: $\mathrm{Pr}\neq 1, \mathrm{Sc}\neq 1$

$$\begin{aligned}\tau &= \frac{t_0\tau'}{\mu Gr} = \left.\frac{\partial u}{\partial y}\right|_{y=0} \\ &= a_4\left[F_3(\mathrm{Pr},a_1,t) - F_3(\mathrm{Pr},a_1,t-1)H(t-1)\right. \\ &\quad - F_3(1,a_0,t) + F_3(1,a_0,t-1)H(t-1)\left.\right] \\ &\quad + a_5\left[F_4(\mathrm{Pr},a_1,0,t) - F_4(\mathrm{Pr},a_1,0,t-1)H(t-1)\right. \\ &\quad - F_4(1,a_0,0,t) + F_4(1,a_0,0,t-1)H(t-1) \\ &\quad - F_4(\mathrm{Pr},a_1,a_2,t) + F_4(\mathrm{Pr},a_1,a_2,t-1)H(t-1) \\ &\quad + F_4(1,a_0,a_2,t) - F_4(1,a_0,a_2,t-1)H(t-1)\left.\right] \\ &\quad + a_6\left[F_4(\mathrm{Sc},\gamma,0,t) - F_4(\mathrm{Sc},\gamma,a_3,t)\right. \\ &\quad - F_4(1,a_0,0,t) + F_4(1,a_0,a_3,t)\left.\right]\end{aligned} \tag{18a}$$

Case II: $\mathrm{Pr}=1, \mathrm{Sc}\neq 1$

$$\begin{aligned}\tau &= \left.\frac{\partial u}{\partial y}\right|_{y=0} \\ &= a_4\left[F_3(1,a_7,t) - F_3(1,a_7,t-1)H(t-1)\right. \\ &\quad - F_3(1,a_0,t) + F_3(1,a_0,t-1)H(t-1)\left.\right] \\ &\quad + a_6\left[F_4(1,a_0,a_3,t) - F_4(1,a_0,0,t)\right. \\ &\quad + F_4(\mathrm{Sc},\gamma,0,t) - F_4(\mathrm{Sc},\gamma,a_3,t)\left.\right]\end{aligned} \tag{18b}$$

Case III: $\mathrm{Pr}\neq 1, \mathrm{Sc}=1$

$$\begin{aligned}\tau &= \left.\frac{\partial u}{\partial y}\right|_{y=0} \\ &= a_4\left[F_3(\mathrm{Pr},a_1,t) - F_3(\mathrm{Pr},a_1,t-1)H(t-1)\right. \\ &\quad - F_3(1,a_0,t) + F_3(1,a_0,t-1)H(t-1)\left.\right] \\ &\quad + a_5\left[F_4(\mathrm{Pr},a_1,0,t) - F_4(\mathrm{Pr},a_1,0,t-1)H(t-1)\right. \\ &\quad - F_4(1,a_0,0,t) + F_4(1,a_0,0,t-1)H(t-1) \\ &\quad - F_4(\mathrm{Pr},a_1,a_2,t) + F_4(\mathrm{Pr},a_1,a_2,t-1)H(t-1) \\ &\quad + F_4(1,a_0,a_2,t) - F_4(1,a_0,a_2,t-1)H(t-1)\left.\right] \\ &\quad + a_8\left[F_5(\gamma,t) - F_5(a_0,t)\right]\end{aligned} \tag{18c}$$

where

$$F_3(z_1,z_2,t) = \left(\frac{1}{2}\sqrt{\frac{z_1}{z_2}} + t\sqrt{z_1 z_2}\right)\times$$
$$\mathrm{erf}\left(\sqrt{z_2 t}\right) + \sqrt{\frac{z_1 t}{\pi}}\exp(-z_2 t)$$

$$F_4(z_1,z_2,z_3,t) = \sqrt{z_1(z_2+z_3)}\times$$
$$\exp(z_3 t)\,\mathrm{erf}\left(\sqrt{(z_2+z_3)t}\right)$$

ISBN: 978-1-61804-304-7

$$F_5(z_1,t)=\sqrt{z_1}\ \mathrm{erf}\left(\sqrt{z_1 t}\right)+\frac{\exp(-z_1 t)}{\sqrt{\pi t}}$$

From the temperature field, the rate of heat transfer is determined and it is given in the form of Nusselt number as

$$\begin{aligned} Nu &= -\frac{\sqrt{\nu t_0}}{(T'_w-T'_\infty)}\left.\frac{\partial T'}{\partial y'}\right|_{y'=0} = -\left.\frac{\partial \theta}{\partial y}\right|_{y=0} \\ &= F_3(\mathrm{Pr},a_1,t)-F_3(\mathrm{Pr},a_1,t-1)H(t-1) \end{aligned} \tag{19}$$

From the concentration field, the rate of mass transfer is determined and it is given in the form of Sherwood number as

$$\begin{aligned} Sh &= -\frac{\sqrt{\nu t_0}}{(C'_w-C'_\infty)}\left.\frac{\partial C'}{\partial y'}\right|_{y'=0} = -\left.\frac{\partial C}{\partial y}\right|_{y=0} \\ &= \sqrt{\mathrm{Sc}\gamma}\ \mathrm{erf}\left(\sqrt{t\gamma}\right)+\sqrt{\frac{\mathrm{Sc}}{t\pi}}\exp(-t\gamma) \end{aligned} \tag{20}$$

2.1 Solution in the Case of Isothermal Plate

The solution for the temperature and velocity variables in the case of isothermal plate is derived as follows:

$$\theta(y,t)=F_2\left(y\sqrt{\mathrm{Pr}},a_1,0,t\right) \tag{21}$$

Case I: $\mathrm{Pr}\neq 1,\mathrm{Sc}\neq 1$

$$\begin{aligned} u(y,t) &= (a_4+a_6)F_2(y,a_0,0,t) \\ &+ a_4\left[F_2(y\sqrt{\mathrm{Pr}},a_1,a_2,t)-F_2(y\sqrt{\mathrm{Pr}},a_1,0,t)\right. \\ &\left.- F_2(y,a_0,a_2,t)\right]+a_6\left[F_2(y\sqrt{\mathrm{Sc}},\gamma,a_3,t)\right. \\ &\left.- F_2(y\sqrt{\mathrm{Sc}},\gamma,0,t)-F_2(y,a_0,a_3,t)\right] \end{aligned} \tag{22a}$$

Case II: $\mathrm{Pr}=1,\mathrm{Sc}\neq 1$

$$\begin{aligned} u(y,t) &= (a_4+a_6)F_2(y,a_0,0,t) \\ &- a_4F_2(y,a_7,0,t)+a_6\left[F_2(y\sqrt{\mathrm{Sc}},\gamma,a_3,t)\right. \\ &\left.- F_2(y\sqrt{\mathrm{Sc}},\gamma,0,t)-F_2(y,a_0,a_3,t)\right] \end{aligned} \tag{22b}$$

Case III: $\mathrm{Pr}\neq 1,\mathrm{Sc}=1$

$$\begin{aligned} u(y,t) &= (a_4+a_8)F_2(y,a_0,0,t) \\ &- a_8F_2(y,\gamma,0,t)+a_4\left[F_2(y\sqrt{\mathrm{Pr}},a_1,a_2,t)\right. \\ &\left.- F_2(y\sqrt{\mathrm{Pr}},a_1,0,t)-F_2(y,a_0,a_2,t)\right] \end{aligned} \tag{22c}$$

The non-dimensional skin-friction and Nusselt number are given by

Case I: $\mathrm{Pr}\neq 1,\mathrm{Sc}\neq 1$

$$\begin{aligned} \tau &= \left.\frac{\partial u}{\partial y}\right|_{y=0} \\ &= a_4\left[F_4(1,a_0,a_2,t)+F_4(\mathrm{Pr},a_1,0,t)\right. \\ &\left.- F_4(\mathrm{Pr},a_1,a_2,t)\right]+a_6\left[F_4(1,a_0,a_3,t)\right. \\ &\left.+ F_4(\mathrm{Sc},\gamma,0,t)-F_4(\mathrm{Sc},\gamma,a_3,t)\right] \\ &- (a_4+a_6)F_4(1,a_0,0,t) \end{aligned} \tag{23a}$$

Case II: $\mathrm{Pr}=1,\mathrm{Sc}\neq 1$

$$\begin{aligned} \tau &= \left.\frac{\partial u}{\partial y}\right|_{y=0} \\ &= a_6\left[F_4(1,a_0,a_3,t)+F_4(\mathrm{Sc},\gamma,0,t)\right. \\ &\left.- F_4(\mathrm{Sc},\gamma,a_3,t)\right]+a_4F_4(1,a_7,0,t) \\ &- (a_4+a_6)F_4(1,a_0,0,t) \\ &+\frac{a_4}{\sqrt{t\pi}}\left[\exp(-a_7t)-\exp(-a_0t)\right] \end{aligned} \tag{23b}$$

Case III: $\mathrm{Pr}\neq 1,\mathrm{Sc}=1$

$$\begin{aligned} \tau &= \left.\frac{\partial u}{\partial y}\right|_{y=0} \\ &= a_4\left[F_4(1,a_0,a_2,t)+F_4(\mathrm{Pr},a_1,0,t)\right. \\ &\left.- F_4(\mathrm{Pr},a_1,a_2,t)\right]+a_8F_4(1,\gamma,0,t) \\ &- (a_4+a_8)F_4(1,a_0,0,t) \\ &+\frac{a_8}{\sqrt{t\pi}}\left[\exp(-t\gamma)-\exp(-a_0t)\right] \end{aligned} \tag{23c}$$

and

$$\begin{aligned} Nu &= -\left.\frac{\partial \theta}{\partial y}\right|_{y=0} \\ &= \sqrt{a_1\ \mathrm{Pr}}\ \mathrm{erf}\left(\sqrt{a_1 t}\right)+\sqrt{\mathrm{Pr}/\,t\pi}\ \exp(-a_1 t) \end{aligned} \tag{24}$$

3 Results and discussion

The numerical values of the velocity and the skin-friction have been computed for different values of the control parameters. The default values for the control parameters are taken as: $\mathrm{Pr}=0.71$(air), $\phi=45^0$, $N=0.2$, $K=0.5$, $M=1$, $R=5$,

ISBN: 978-1-61804-304-7

$Q = -0.5$ (heat generation), $\mathrm{Sc} = 0.6$ (water vapor), $\gamma = 1$ and $t = 0.6$. In order to highlight the influence of ramped wall temperature distribution on free convection flow along an infinite inclined plate, the present study has also been compared with that of the isothermal plate. The variation of the velocity profiles with time is shown in Fig. 1. It is observed that the velocity increases as the time progresses and this increase in velocity profiles is more in the isothermal case when compared to the ramped temperature case. This should be expected since the buoyancy force gradually increases with time in the case of ramped wall temperature as compared to the isothermal case. Further, the location of the peak velocity is moving away from the plate as the time progresses.

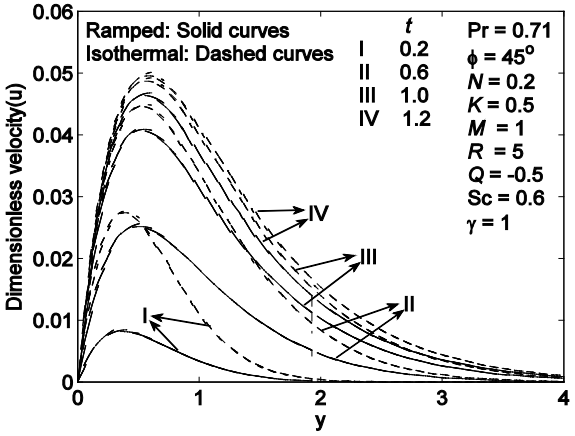

Fig. 1 Velocity profiles at different t

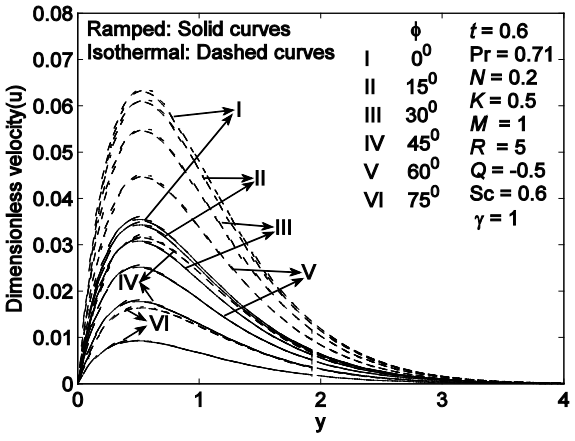

Fig.2 Velocity profiles at different ϕ

The velocity variation with the inclination angle is shown in Fig. 2. It is observed that the velocity decreases with increasing inclination angle for both isothermal and ramped temperature cases. This is due to the decrease in the buoyancy force with increasing inclination angle from vertical. The velocity profiles are lower in the case of ramped wall temperature than that of the isothermal case.

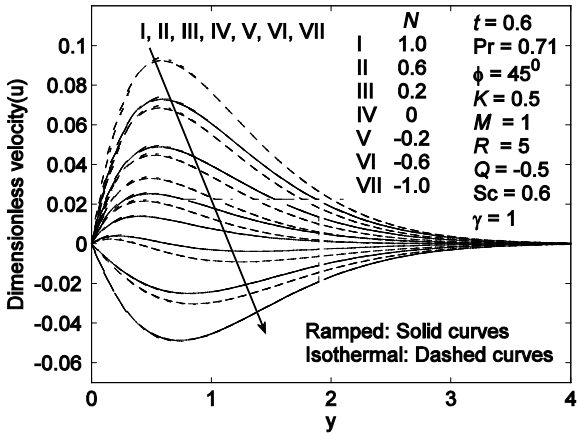

Fig. 3 Velocity profiles at different N

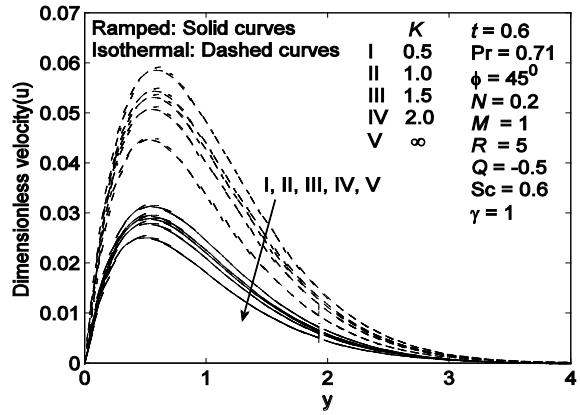

Fig. 4 Velocity profiles for different K

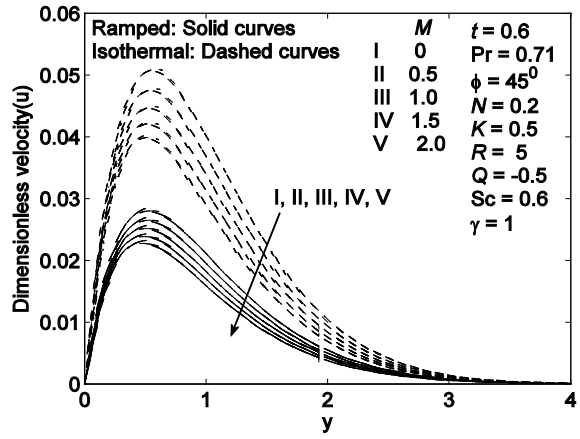

Fig. 5 Velocity profiles for different M

The velocity profiles are shown in Fig. 3 for different values of the buoyancy ratio parameter N when other parameters are fixed at default values. It can be seen that the velocity increases with increasing values of N for an aiding flow $(N > 0)$.

ISBN: 978-1-61804-304-7

The reason is that the mass buoyancy force acts in the same direction as the thermal buoyancy force. In the case of an opposing flow ($N<0$), the velocity decreases with increasing opposing buoyancy force. The reason is that the mass buoyancy force acts opposite to the thermal buoyancy force. Again one can see that fluid velocity is lower in the case of ramped temperature plate than in the case of isothermal temperature. Physically this true because in ramped temperature case heating takes place gradually when compared to isothermal temperature case.

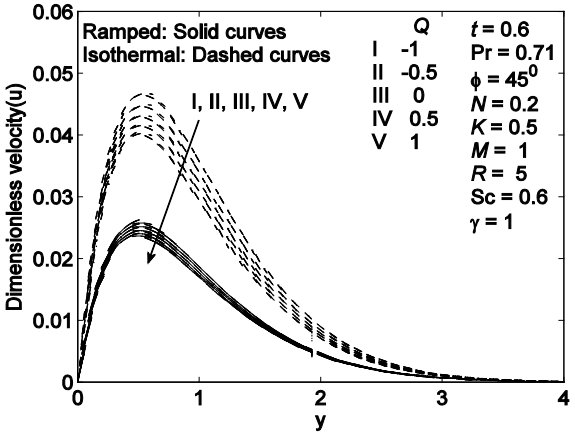

Fig. 6 Velocity profiles for different Q

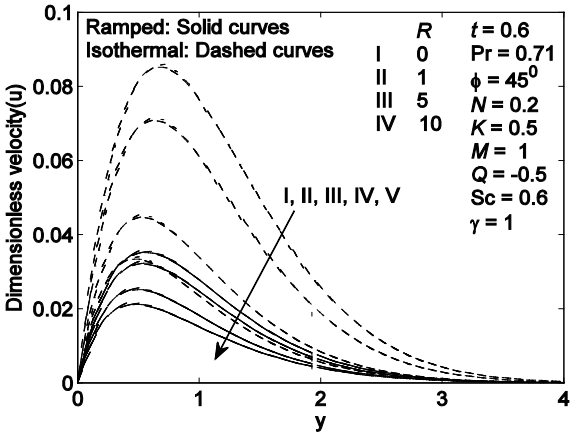

Fig. 7 Velocity profiles for different R

The velocity profiles are shown in Fig. 4 for different values of the permeability parameter K when other control parameters are fixed at the default values. It is observed that the velocity decreases with decreasing values of K for both isothermal and ramped temperature cases. Small values of K refer to cases when the medium is almost rigid and $K\to\infty$ refer to the case of absence of porous medium. It is also observed that the fluid velocity is higher in the case of isothermal temperature when compared to ramped temperature case for fixed value of the permeability parameter K.

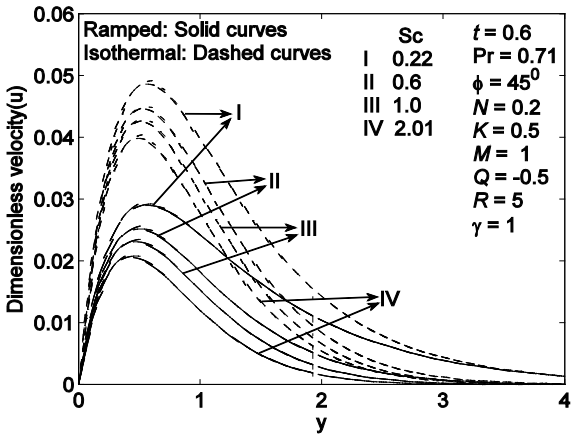

Fig. 8 Velocity profiles for different Sc

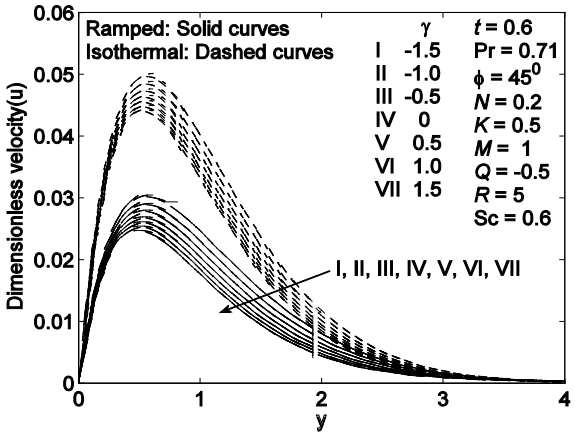

Fig. 9 Velocity profiles for different γ

The effect of magnetic field on velocity profiles is depicted in Fig. 5. From this figure, it can be seen that in both isothermal and ramped temperature cases the velocity decreases with increasing value of the magnetic field parameter. The presence of magnetic field in an electrically conducting fluid introduces a force called Lorentz force, which acts against the flow if the magnetic field is applied in the normal direction to the flow. This type of resisting force slow down the fluid velocity as observed in Fig. 5. Further it is noticed that velocity is lower in the ramped temperature case as compared to isothermal temperature case. The influence of heat generation ($Q<0$) or heat absorption ($Q>0$) on the velocity field is presented in Fig. 6 for both isothermal and ramped temperature cases. The presence of heat generation in the boundary layer generates thermal energy which causes to increase the fluid temperature and

ISBN: 978-1-61804-304-7

thereby produces an increase in the fluid velocity due to increasing buoyancy effect. An opposite trend is observed in the case of heat absorption. It is seen that the fluid velocity is lower in the case ramped temperature plate as compared to that of isothermal plate for both heat generation and absorption.

The effect of thermal radiation on the velocity profiles is depicted in Fig. 7 for both ramped and isothermal temperature cases. Increasing the thermal radiation parameter R produces a significant decrease in the fluid temperature. This result is expected qualitatively from the definition of R given in eq. (8). The effect of radiation parameter is to decrease the rate of energy transport to the fluid and thereby decreasing the temperature of the fluid. This decrease in the fluid temperature causes the fluid velocity to decrease due to the reduced buoyancy effect.

The variation of the velocity field is illustrated in Fig. 8 for different values of the Schmidt number when the other parameters are fixed at their default values for both isothermal and ramped temperature cases. This figure clearly indicates that the velocity decreases with increasing values of the Schmidt number. Further it is noticed from this figure that the velocity profiles are lower in the case of ramped temperature than in the case of isothermal temperature case.

The effect of chemical reaction parameter γ ranging from non-destructive $(\gamma < 0)$ to destructive $(\gamma > 0)$ chemical reactions on the velocity profiles is depicted in Fig. 9 for isothermal and ramped temperature cases. The presence of destructive chemical reaction has tendency to decrease the solute concentration which causes a slight decrease in the fluid velocity due to reduced mass buoyancy force. For non-destructive chemical reactions, the exact opposite effect is predicted in fluid velocity.

The skin-friction variation with dimensionless time at different values of inclination angle ϕ is depicted in Fig.10 when other parameters are fixed at the default values. It is observed that an increase in the value of ϕ decreases the skin-friction for both ramped temperature and isothermal plate cases. This should be expected because the fluid velocity decreases with increasing the inclination angle for both ramped temperature and isothermal plate cases. The variation of the skin-friction with time for different values of buoyancy ratio parameter N is shown in Fig.11. It is observed from this figure that the skin-friction increases with increasing aiding buoyancy force whereas it decreases with increasing opposing buoyancy force for both ramped temperature and isothermal cases. It is also observed that the skin-friction is negative in the ramped temperature case with increasing value of opposing buoyancy force due to flow separation at the plate.

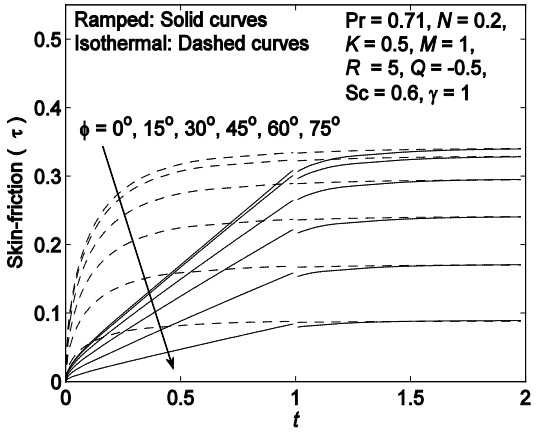

Fig. 10 Skin-friction variation for different ϕ

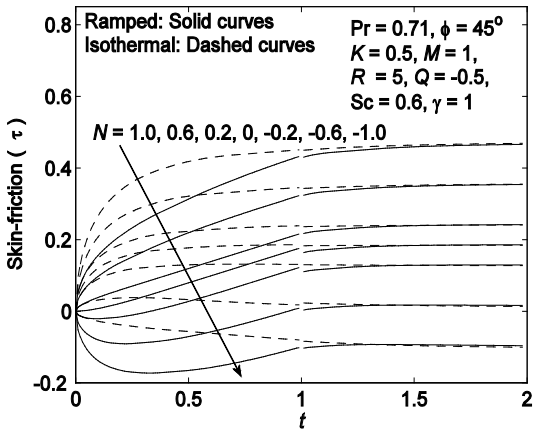

Fig. 11 Skin-friction variation for different N

The skin-friction profiles for different values of the permeability parameter K against time are plotted in Fig.12 for both ramped temperature and isothermal plate. It is observed that an increase in the value of K increases the skin-friction. That is, increasing permeability of the porous medium decreases the skin-friction. The variation of skin friction for different values of heat generation or absorption parameter Q as a function of time is plotted in Fig. 13 for both ramped and isothermal cases. It is noticed that the skin-friction increases with increasing heat generation while it decreases with increasing heat absorption in the boundary layer. This is due to the increase in the momentum boundary layer thickness in the presence of heat

ISBN: 978-1-61804-304-7

generation while it decreases in the presence of heat absorption.

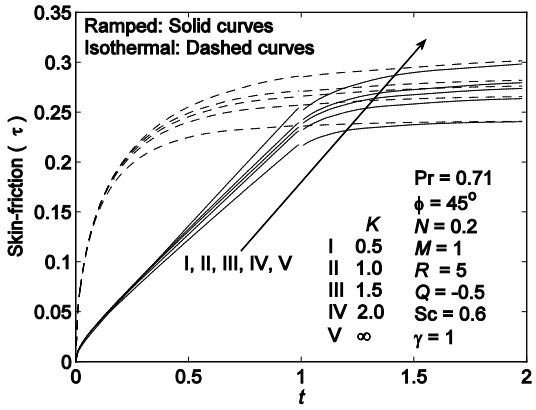

Fig. 12 Skin-friction variation for different *K*

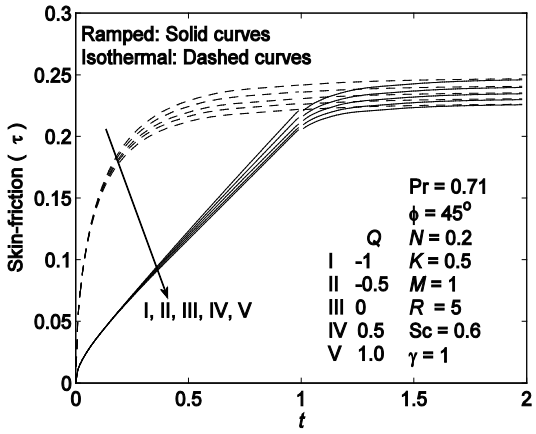

Fig. 13 Skin-friction variation for different *Q*

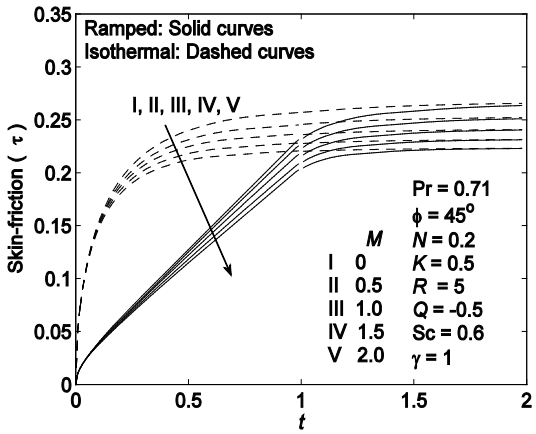

Fig. 14 Skin-friction variation for different *M*

The variation of skin-friction with time for different values of magnetic field parameter *M*, radiation parameter *R*, and Schmidt number Sc is shown in Figs. 14 – 16, respectively, for both ramped temperature and isothermal temperature of the plate. It observed that the increasing values of *M*, *R* and Sc decreases the skin-friction in both the cases. This is due to the decrease in the fluid velocity with increasing values of *M*, *R* and Sc for both ramped temperature and isothermal cases. It is interesting to note that the skin-friction decreasingly pronounced more with radiation parameter *R* as compared to the magnetic field parameter *M* and Schmidt number Sc.

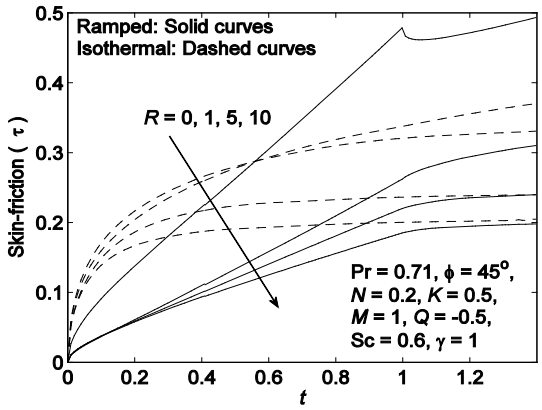

Fig. 15 Skin-friction variation for different *R*

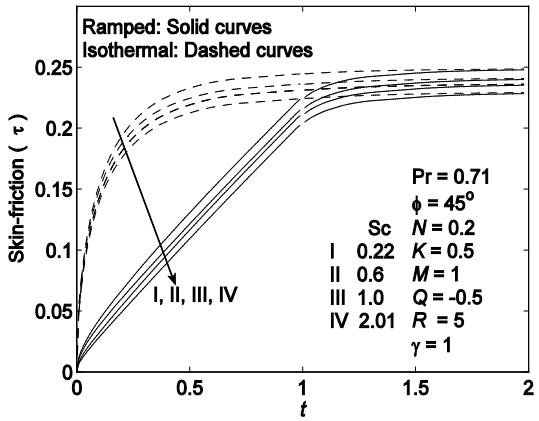

Fig. 16 Skin-friction variation for different Sc

The skin friction variation against time is plotted for different values of the chemical reaction parameter γ in Fig. 17 for both ramped and isothermal cases. It is clear that the skin-friction increases with increasing non-destructive chemical reaction due to increasing fluid velocity whereas the skin-friction decreases with increasing destructive chemical reaction due the decrease in the fluid velocity for both cases. From Figs. 10 – 17 it is important to notice that the skin-friction is greater

ISBN: 978-1-61804-304-7

in the case of isothermal plate as compared to the ramped temperature plate for small values of time and at large values of time the skin-friction attains the steady state value in both the cases. Further, the skin-friction attains the steady state value early in the case of isothermal plate as compared to the ramped temperature plate. This should be expected since heating of the fluid is takes place more gradually in the case of ramped temperature of the plate as compared to the case of isothermal plate.

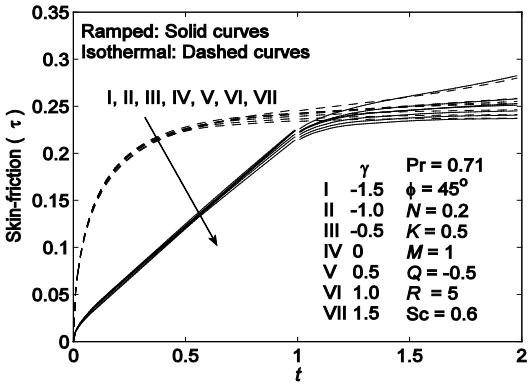

Fig. 17 Skin-friction variation for different γ

4 Conclusion

The problem of unsteady natural convection heat and mass transfer past an infinite inclined plate in a porous medium with ramped wall temperature is studied analytically under the influence of magnetic field, thermal radiation, heat generation or absorption, and destructive or non-destructive chemical reaction. Closed form analytical solutions to the dimensionless governing partial differential equations are obtained using the Laplace transform technique without any restriction. The numerical values of velocity and skin-friction have been computed from the analytical solutions for different values of control parameters. The fluid velocity and skin-friction obtained for the ramped temperature plate have been compared with that for the case of an isothermal plate. It is found that the fluid velocity and skin-friction are lower in the case of ramped wall temperature boundary condition than those obtained for the case of isothermal boundary condition. The present results will have immediate relevance in the design of solar energy collectors, geothermal systems, cooling of electronic equipment and in the design of chemical processing equipment.

Acknowledgements

The authors greatly acknowledge Universiti Teknologi PETRONAS for providing facilities and the Ministry of Higher Education (MOHE), Malaysia for financial support under the Fundamental Research Grant Scheme (FRGS/1/2012/TKO1/ UTP/02/06).

References:

[1] S. Lee and M. M. Yovanovich, Laminar Natural Convection from a Vertical Plate with Step Change in Wall Temperature, *Journal of Heat Transfer*, Vol. 113, 1991, pp. 501–504.

[2] A. A. Hayday, D. A. Bowlus and R. A. McGraw, Free Convection from a Vertical Flat Plate with Step Discontinuities in Surface Temperature, *Journal of Heat Transfer,* Vol. 89, No. 3, 1967, pp. 244–250.

[3] T. T. Kao, Laminar Free Convective Heat Transfer Response along a Vertical Flat Plate with Step Jump in Surface Temperature, *Letters in Heat Mass Transfer*, Vol. 2, No. 5, 1975, pp. 419–428.

[4] P. Chandran, N. C. Sacheti and A. K. Singh, Natural Convection Near a Vertical Plate with Ramped Wall Temperature, *Heat Mass Transfer*, Vol. 41, 2005, pp. 459–464.

[5] M. Narahari and B. K. Dutta, Effects of Mass Transfer and Free-Convection Currents on the Flow near A Moving Vertical Plate with Ramped Wall Temperature, In: Proceedings of the *ASME 2009 heat transfer summer conference*, July 19–23, San Francisco, USA. Paper no. HT2009-88045.

[6] M. Narahari and V. R. Raghavan, Natural Convection Flow in Vertical Channel Due to Ramped Wall Temperature at One Boundary, In: Proceedings of the *ASME 2009 heat transfer summer conference*, July 19–23, San Francisco, USA. Paper no. HT2009-88046.

[7] M. Narahari, O. A. Beg and S. K. Ghosh, Mathematical Modeling of Mass Transfer and Free Convection Current Effects on Unsteady Viscous Flow with Ramped Wall Temperature, *World Journal of Mechanics*, Vol. 1, 2011, pp. 176–184.

[8] S. C. Saha, C. Patterson and C. Lei, Natural Convection Boundary-Layer Adjacent to an Inclined Flat Plate Subject to Sudden and Ramp Heating, *International Journal of Thermal Sciences*, Vol. 49, 2010, pp. 1600–1612.

[9] A. K. Tiwari, Combined Effect of Magnetic Field and Ramped Temperature in a Porous

Medium Bounded by a Vertical Wall, *Heat and Technology*, Vol. 27, No. 2, 2009, pp. 111–117.

[10] R. K. Singh and A. K. Singh, Transient MHD Free Convective Flow Near a Semi-Infinite Vertical Wall Having Ramped Temperature, *International Journal of Applied Mathematics and Mechanics*, Vol. 6, No. 5, 2010, pp. 69–79.

[11] G. S. Seth, Md. S. Ansari and R. Nandkeolyar, MHD Natural Convection Flow with Radiative Heat Transfer Past an Impulsively Moving Plate with Ramped Wall Temperature, *Heat Mass Transfer*, Vol. 47, 2011, pp. 551–561.

[12] V. Rajesh**,** Chemical Reaction and Radiation Effects on the Transient MHD Free Convection Flow of Dissipative Fluid Past an Infinite Vertical Porous Plate with Ramped Wall Temperature, *Chemical Industry & Chemical Engineering*, Vol. 17, No. 2, 2011, pp. 189-198.

[13] D. Kalidas, Magnetohydrodynamics Free Convection Flow of a Radiating and Chemically Reacting Fluid Past an Impulsively Moving Plate with Ramped Wall Temperature, *Journal of Applied Mechanics*, Vol. 79, 2012, pp. 061017-1-11.

[14] M. Narahari, Transient Free Convection Flow between Long Vertical Parallel Plates with Ramped Wall Temperature at One Boundary in The Presence of Thermal Radiation and Constant Mass Diffusion, *Meccanica,* Vol. 47, 2012, pp.1961–1976.

[15] Samiulhaq, I. Khan, F. Ali and S. Shafie, MHD Free Convection Flow in a Porous Medium with Thermal Diffusion and Ramped Wall Temperature, *Journal of the Physical Society of Japan*, Vol. 81, 2012, pp. 044401-1-9.

[16] M. Narahari and S. A. Sulaiman, Thermal Radiation Effects on Unsteady MHD Natural Convection Flow Past an Infinite Inclined Plate with Ramped Temperature, *Advanced Science Letters,* Vol. 19, No. 1, 2013, pp. 296-300.

[17] R. Nandkeolyar, M. Das and P. Sibanda, Unsteady Hydromagnetic Heat and Mass Transfer Flow of a Heat Radiating and Chemically Reactive Fluid Past a Flat Porous Plate with Ramped Wall Temperature, *Mathematical Problems in Engineering*, Vol. 2013, Article ID 381806, 2013, pp. 1-12.

[18] Z. Ismail, A. Hussanan, I. Khan and S. Shafie, MHD and Radiation Effects on Natural Convection Flow in a Porous Medium Past an Infinite Inclined Plate with Ramped Wall Temperature: An exact analysis, *International Journal of Applied Mathematics and Statistics*, Vol. 45, No. 15, 2013, pp. 77-86.